



Limonium tetragonum Reduces Osteoclast Formation and Resorption through Mitogen-activated Protein Kinase-c-Fos-NFATc1 Signaling Pathways

Saroj Kumar Shrestha^{1†}, Hwangeui Cho^{1†}, Se-woong Kim¹, Jong-Sik Jin², and Yunjo Soh^{1,*}

¹School of Pharmacy and Institute of New Drug Development, Jeonbuk National University, Jeon-Ju 54896, Republic of Korea

²Department of Oriental Medicine Resources, and LED Agri-bio Fusion Technology Research Center, Jeonbuk National University, Iksan 54596, Republic of Korea

Abstract – Osteoporosis is caused by an imbalance of osteoclasts and osteoblasts, and the major treatment technique for treating osteoporosis is to reduce the activity of osteoclastic bone resorption. *Limonium tetragonum* (LT) is a medicinal plant that contains bioactive molecules with anti-inflammatory and anti-cancer properties. Its effects on osteoclastogenesis, however, remain unclear. *Limonium tetragonum* extract (LTE) was examined for its inhibitory effect on osteoclastogenesis by TRAP and pit formation assay. As a result, LTE also significantly reduced TRAP formation, the capability to resorb calcium phosphate-coated plates, and F-actin ring formation. LTE reduced RANKL-induced activation of the MAPKs ERK, JNK, and p38 and the production of the transcription factors c-Fos and NFATc1 required for osteoclastogenesis. LTE also reduced the expression of osteoclastogenesis-related genes such as matrix metalloproteinase-9, tartrate-resistant acid phosphatase, and receptor activator of NF- κ B. These findings suggest that LTE might be a promising treatment option for bone disorders caused by aberrant osteoclast production and function.

Keywords – *Limonium tetragonum*, osteoclastogenesis, RANKL, TRAP, bone loss, NFATc1, Cathepsin K

Introduction

The bone-resorbing multinucleated giant cells known as osteoclasts are formed from monocyte/macrophage lineage cells.¹ However, destructive bone illnesses such as osteoporosis, periodontitis, rheumatoid arthritis, and metastatic malignancies produce an imbalance of bone homeostasis due to excessive osteoclast development.^{2,3}

Two important cytokines, macrophage colony-stimulating factor (M-CSF) and receptor activator of nuclear factor- κ B ligand, govern osteoclast development (RANKL).⁴ RANKL belongs to the tumor necrosis factor (TNF)-superfamily (TNFSF11) and binds to a membrane receptor called receptor activator of nuclear factor-B (RANK), which belongs to the TNF receptor superfamily (TNFRSF11A).⁵ TNF receptor-associated factors 6 (TRAF6) is activated by the RANK/RANKL axis in hematopoietic precursor cells, which subsequently controls numerous downstream signaling pathways such as mitogen-activated protein

kinase (MAPKs), nuclear factor- κ B (NF- κ B), and PI3K/AK.^{6,7} The expression of the nuclear factor of activated T cells (NFATc1), a key transcription factor for osteoclastogenesis, is eventually achieved due to this advancement.⁸ By regulating various osteoclast-specific genes, including tartrate-resistant acid phosphatase (TRAP), Cathepsin K (Cts K), matrix metalloproteinase-9 (MMP-9), and dendritic cell-specific transmembrane protein (DC-STAMP), NFATc1 plays a vital role in osteoclast development and function.^{9,10} As a result, the mechanism underpinning RANKL or its signaling pathways in osteoclast production might have important therapeutic implications for bone resorption illnesses such as osteoporosis, periodontitis, and osteoarthritis.

Limonium tetragonum is a salt-tolerant biennial plant in the Plumbaginaceae family known as the ‘halophytic carrot’ owing to its long straight root resembling a carrot. It is found widely in salt marshes and on muddy seashores alone in the southwestern coastal areas of South Korea. According to reports, *L. tetragonum* has anti-oxidative capabilities and has several positive effects on a variety of diseases, including high-fat diet-induced obesity,¹¹ alcohol-induced liver damage in mice,¹² and diethylnitrosamine-induced liver fibrosis in rats.¹³ *In-vitro* investigations have

[†]These authors equally contributed to this work.

*Author for correspondence
Dr. Yunjo Soh, Department of Pharmacology, School of Pharmacy, Jeonbuk National University, Jeon-Ju 561-756, Korea
Tel: +82-63-270-4038; E-mail: ysoh@jbnu.ac.kr

shown that *L. tetragonum* extract inhibits matrix metalloproteinase activity in HT1080 fibrosarcoma cells¹⁴ and the proliferation of HSC-T6 hepatic stellate cells and B16-F10 melanoma cells.^{14,15} From the ethyl acetate soluble fraction of *L. tetragonum* extract, many bioactive flavonoids, flavonoid glycosides, and catechins that may have pharmacological effects have been identified. LC-MS study shows that LTE contains epicatechin, (-)-epigallocatechin-3-gallate, myricetin-3-*O*- β -D-galactopyranoside, myricetin-3-*O*- α -L-rhamnopyranoside, myricetin-3-*O*-(2"-*O*-galloyl)- α -L-rhamnopyranoside, and myricetin-3-*O*-(3"-*O*-galloyl)- α -L-rhamnopyranosid¹¹. In this study, we prepared the 30% ethyl alcohol extract of *L. tetragonum* (LTE) using plants cultivated in a smart-farm factory using LED grow lights, as opposed to those that grew naturally along the coast of South Korea. The mechanism of LTE has not been studied on RANKL-induced osteoclast differentiation activity. In this study, we examined the effect of LTE on osteoclastogenesis in RAW 264.7 cells *in-vitro*.

Experimental

Materials – The *Limonium tetragonum* was identified by Suk-Kyu Kim (Halopharm Co., Iksan, Korea) as previously described.¹⁶ It was dissolved in distilled water and diluted to the required working concentration. Dulbecco's modified Eagle's medium (DMEM), fetal bovine serum (FBS), penicillin, and streptomycin were purchased from Gibco. The cell counting kit-8 (CCK-8) was obtained from Dojindo Molecular Technologies. Leukocyte Acid Phosphatase (TRAP) kit was purchased from Sigma Aldrich. Calcium phosphate (CaP) coated plates were obtained from Cosmo Bio (Tokyo, Japan). Recombinant soluble mouse RANKL was purchased from R&D (R&D systems, MN). Primary and secondary antibodies were obtained from Cell signaling technology and Santa Cruz biotechnology.

Preparation of LTE – After being cleaned, the LT leaf was left in an oven set to 60°C for the whole night. Using a reflux condenser, the dried leaf of LT was extracted for one hour at 100°C in hot water with a solid-to-liquid ratio of 1:25 (w/v). Before being used, the extract was lyophilized (batch process), filtered using Whatman filter paper No. 1, and kept at 4°C. The dried extract yielded a proportion of 28.2% w/w.¹¹

Cell culture – The American Type Culture Collection (ATCC; Rockville, MD, USA) provided RAW 264.7 cells, which were grown in DMEM supplemented with 10% heat-inactivated FBS and 1% streptomycin/penicillin at 37°C in a humidified incubator under 5% CO₂.

Cell viability assay – According to the manufacturer's instructions, a cytotoxicity experiment was done using the Cell Counting Kit-8 to assess the effect of LTE on the viability of RAW 264.7 cells. RAW 264.7 cells (5×10^3 cells/well) were planted for 16 hours in 96-well plates. The cells were subsequently treated for 1, 3, or 6 days with varying doses of LTE or vehicle in each well. A microplate reader (BioTek, Power wave HT) was used to detect optical density at 540 nm after incubating the cells with CCK-8 solution for 2 hours. The data were computed as mean \pm S.D. from triplicate wells, and cell viability was given as a percentage of the control.

Osteoclast formation and TRAP staining – RAW 264.7 cells at a density of 1×10^3 cells/well for osteoclast development. Cells were kept alive in the presence of 50 ng/mL of RANKL and 1, 5, and 10 μ g/mL of LTE. For 6 days, the culture medium was replaced every 2–3 days. According to the manufacturer's instructions, the cells were fixed in 4 % paraformaldehyde for 10 minutes and stained with a tartrate-resistant acid phosphatase (TRAP) staining kit. A light microscope (IX71; Olympus, Tokyo, Japan) was used to count TRAP-positive multinucleated cells (TRAP+ MNCs) as osteoclast-like cells.

Pit formation assay – A bone Resorption Test Kit (#CSF-BRA- 48 KIT, Cosmo Bio, Tokyo, Japan) covered with a calcium phosphate (CaP) plate was used to perform the bone resorption pit assay. 5×10^3 RAW 264.7 cells were seeded in calcium phosphate (CaP) coated 48-well plates with 50 ng/mL RANKL and various doses of LTE (5 to 20 μ g/mL) for 6 days. Every two days, the culture media was replaced. The pit area was assessed using Image J after the cells were stained using a TRAP staining kit.

Actin ring formation – RAW 264.7 were seeded in 96 well plates at a density of 4×10^3 cells/well, in triplicate, in DMEM containing 50 ng/mL RANKL along with LTE of 20 μ g/mL for 6 days to evaluate F-actin ring formation. Cells were washed with $1 \times$ PBS, fixed with 4% paraformaldehyde for 15 min, and $1 \times$ PBS was again used to wash the cells. Then, 0.1% Triton was added for 1 min to permeabilise cells. $1 \times$ Red Fluorescent Phalloidin Conjugate was added for 60 min, and nuclear staining was performed by adding 4', 6-diamidino-2-phenylindole (DAPI). Finally, F-actin ring formation was observed using a fluorescence microscope (Olympus).

RNA extraction and reverse-transcription-real time polymerase chain reaction – In the presence of 50 ng/mL RANKL, RAW 264.7 cells were seeded at a density of 1×10^5 cells per well in a 6-well plate and treated with LTE (1, 5, and 10 μ g/mL) or vehicle. For 3 days, the

culture medium was replaced every 2 days. Total RNA was acquired from RAW 264.7 cells using TRIZOL reagents. The superscript synthesis system (Invitrogen) was used to synthesize cDNA using 1 µg of RNA. A 20 µL monoplex reaction contained 10 µL of SsoAdvanced™ Universal SYBR Green supermix (BIO-RAD), 1 µL of each primer (0.3 µM final concentration each), 1 µL of the cDNA (0.1 µM final concentration), 8 µL of nuclease-free water. Thermal cycling was run on a Step-two Plus RT-PCR thermal cycler (BIO RAS) with the following cycle parameters: 95°C for 30 sec for polymerase activation and DNA denaturation, 98°C for 15 s, and then 40 cycles of 95°C for 5 s and 60°C for 30 s. The following primers were used in this study: β-actin, 5'-tttacaat gagctgcgtgt-3' and 5'-ctcatagctcttccagg-3'; TRAP, 5'-ctgctggcctacaaatcat-3' and 5'-ggtagtaaggctggggaag-3' Cathepsin K, 5'-aggcggctatatgaccactg-3 and 5'-ccgagccaagagag catatc-3'; MMP-9, 5'-cgtcgtgatccccactact-3', and 5'-agag tactgctgccagga-3'; RANK, 5'-aaaccttgaccaactgcac-3', and 5'-accatctctctcccagtg-3'; c-Fos, 5'-atggctctctgtcaaac-3', and 5'-ggctccaaaataaaactcca-3'; NFATc1, 5'-gggtcagtg gaccgaagat-3', and 5'-aggtgggtgaagactgaagg-3'. Bioneer provided PCR primers for RT-PCR, and all reactions were run in triplicate.

Western blot analysis – RAW264.7 cells were plated at a density of 5×10^5 cells per well in a DMEM medium

in a 60 mm cell culture dish. The cells were lysed using radioimmunoprecipitation (RIPA) buffer [20 mmol/mL Tris-HCL pH 7.4, 150 mmol /mL NaCl, 1 mmol /mL EDTA, 1 percent Triton-X100, 1 percent sodium deoxycholate, 0.1 percent SDS, 1 mmol /mL PMSF, and 1 × protease inhibitor cocktail, iNtRON] after 24 hours and treated with RANKL SDS-PAGE was used to separate equal quantities of proteins, which were then transferred to PVDF nitrocellulose membranes (Bio-Rad). The membranes were blocked for 1 hour at room temperature with 5% nonfat skim milk before probing with specified primary antibodies at 4°C. The membranes were probed for 1 hour with horseradish peroxidase-conjugated secondary antibodies after 24 hours. The Clarity Western ECL Substrate kit (Bio-Rad) was used to detect immunoreactive bands, and Image J software was used to do quantitative analysis.

Statistical analysis – The data were analyzed using the GraphPad Prism 5.0 statistical program (GraphPad Software), one-way ANOVA with Tukey's Multiple Comparison Test. P-values less than 0.05 were deemed statistically significant differences.

Results and Discussion

RAW 264.7 cells were used to examine the effect of

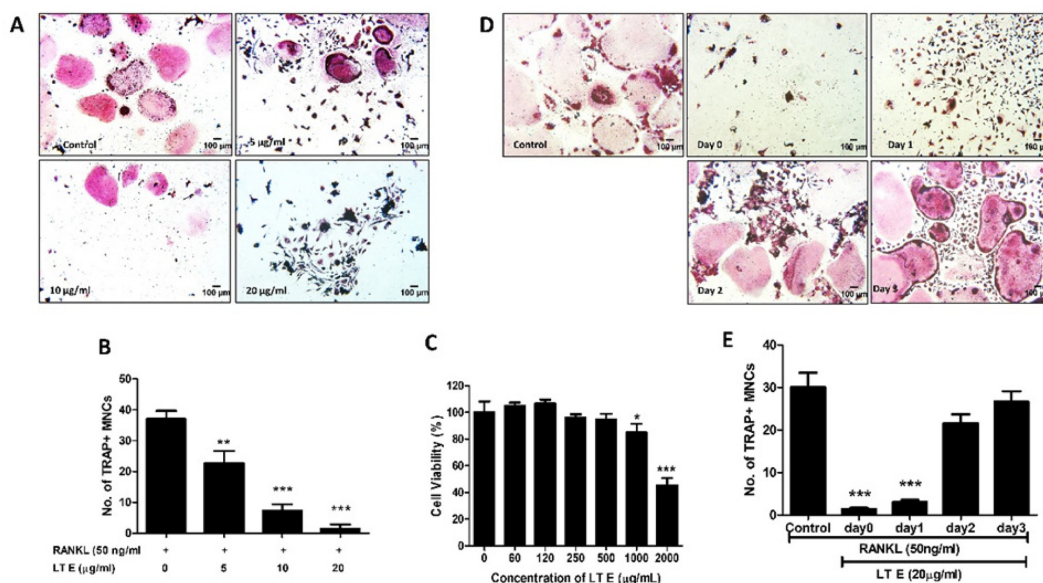


Fig. 1. LTE attenuates the osteoclast differentiation in RAW 264.7 cells in a concentration and time-dependent manner. (A) 50 ng/mL RANKL was added to RAW 264.7 cells in the presence of LTE for 5 days. Cells were fixed according to the protocol for TRAP staining. (B) TRAP+ multinucleated cells with 3 or more nuclei were counted. The percentage relative to the RANKL-treated group is shown. (C) the effect of LTE on cell viability was measured using CCK-8 assay, and the relative percentage was compared with the untreated group. (D, F) RAW 264.7 cells were incubated with given concentrations of RANKL for 6 days and LTE for 3 days, respectively, and the number of TRAP+ MNC was decreased on different days relative to the RANKL-treated group. * $p < 0.05$, ** $p < 0.01$ and *** $p < 0.001$ vs RANKL treated as control. All the data are represented as mean \pm S.D. with $n = 3$.

LTE in a dose and time-dependent manner in the *in vitro* osteoclastogenesis model that was treated with RANKL and increasing LTE doses. RAW 264.7 cells were incubated with different concentrations of LTE in the presence of 50 ng/mL RANKL for 6 days. 5, 10, and 20 $\mu\text{g/mL}$ concentrations of LTE significantly inhibit the osteoclast formation compared to the RANKL-only treated group (Fig. 1A). Further, different concentrations of LTE (up to 500 $\mu\text{g/mL}$) do not show any toxicity effect on RAW 264.7 cells (Fig. 1C) for 72 h. RAW264.7 cells were treated with LTE at different points (0-3 days) and incubated for 6 days to examine the step of maturation of osteoclastogenesis (e.g., proliferation, differentiation, polarisation, and resorption) LTE is involved in. LTE markedly inhibited the osteoclast formation on day 0 and day 1 of LTE treatment but not on day 2 and day 3, indicating that LTE acts on nascent osteoclasts but not on mature osteoclasts. Increased RANKL activity causes osteoclast development, which leads to bone resorption and illnesses such as osteoporosis, Paget's disease, rheumatoid arthritis, and bone metastases.¹ As a result, inhibiting osteoclast development and function may aid in preventing or treating osteoclast-related disorders.

Since LTE inhibits osteoclastogenesis, we next examined the effect of LTE on bone resorption activity on calcium-coated plates. RAW 264.7 cells were cultivated on calcium-coated plates in the presence of 50 ng/mL RANKL for 6 days. Fig. 2A shows that RANKL-induced cells exhibited more resorbed area, but the treatment of 10 and 20 $\mu\text{g/mL}$ LTE significantly reduced the area of bone resorption (Fig. 1A, B). Actin ring was formed when osteoclast precursor cells were differentiated into mature osteoclast, indicating osteoclast maturation during osteoclastogenesis.¹⁷ Furthermore, RANKL was added to RAW

264.7 cells along with 20 $\mu\text{g/mL}$ LTE for 6 days, and F-actin ring formation was evaluated. RANKL treated group clearly showed the F-actin ring formation, whereas 20 $\mu\text{g/mL}$ LTE significantly repressed F-actin ring formation (Fig. 2C). These results suggest LTE inhibits bone resorption and F-actin ring formation, which is essential for the formation of mature osteoclasts.

Next, we looked at whether LTE influenced the expression of TRAP, Cts K, MMP-9, and RANK on RAW 264.7 cells, which are all osteoclast-specific genes. RANKL, a critical factor that governs the activity and survival of mature osteoclasts, can promote osteoclast differentiation from the macrophage.¹⁸ RANKL significantly enhanced osteoclast differentiation-related genes¹ compared to the control group, as revealed by RT-qPCR results. However, at 10 or 20 $\mu\text{g/mL}$ concentrations, LTE dramatically reduced TRAP, MMP-9, Cts K, and RANK mRNA expression (Fig. 3A-D). According to these findings, LTE can block the activation of osteoclast-related genes in RANKL-induced RAW 264.7 cells.

We looked into MAPKs, an essential signaling route during osteoclast development,¹⁹ to learn more about the molecular mechanism of LTE on RANKL-induced RAW 264.7 cells. The activation of the MAPK pathway occurs when RANKL binds to its receptor RANK. Furthermore, RANK/RANKL interaction enhances particular intracellular signaling transduction pathways of MAPKs, such as ERK, JNK, and p38, which are essential in osteoclastogenesis.²⁰ ERK activity is linked to cell survival but not to resorption function in osteoclasts, while p38 and JNK are phosphorylated in response to RANKL activation.²¹ In RANKL-induced osteoclasts, the phosphorylation of ERK1/2, JNK, and p38 proteins was up-regulated within 15 min compared to the control group. However, in LTE-treated

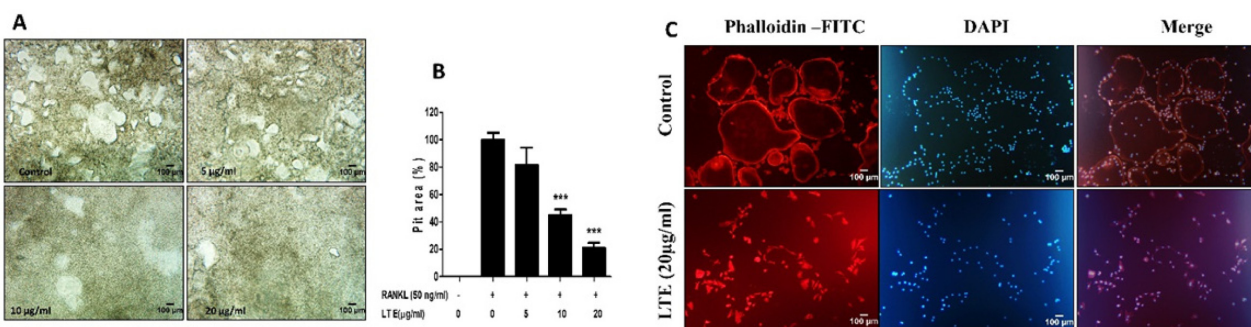


Fig. 2. LTE attenuates pit area formation and disrupts the F-actin ring structure. (A) RAW 264.7 cells were seeded in CaP-coated 48-well plates and treated with 50 ng/mL RANKL in the presence of the indicated concentrations of LTE for 6 days. After 6 days, the cells were removed, and (B) and pit areas were observed. (C) 50 ng/mL RANKL was added to RAW 264.7 cells in the presence of the indicated concentrations of LTE for 5 days. After 5 days, the cells were fixed, and F-actin ring formation was observed using a fluorescence microscope (Scale bar, 100 μm). * $p < 0.05$, ** $p < 0.01$ and *** $p < 0.001$ vs RANKL treated as control. All the data are represented as mean \pm S.D. with $n = 3$.

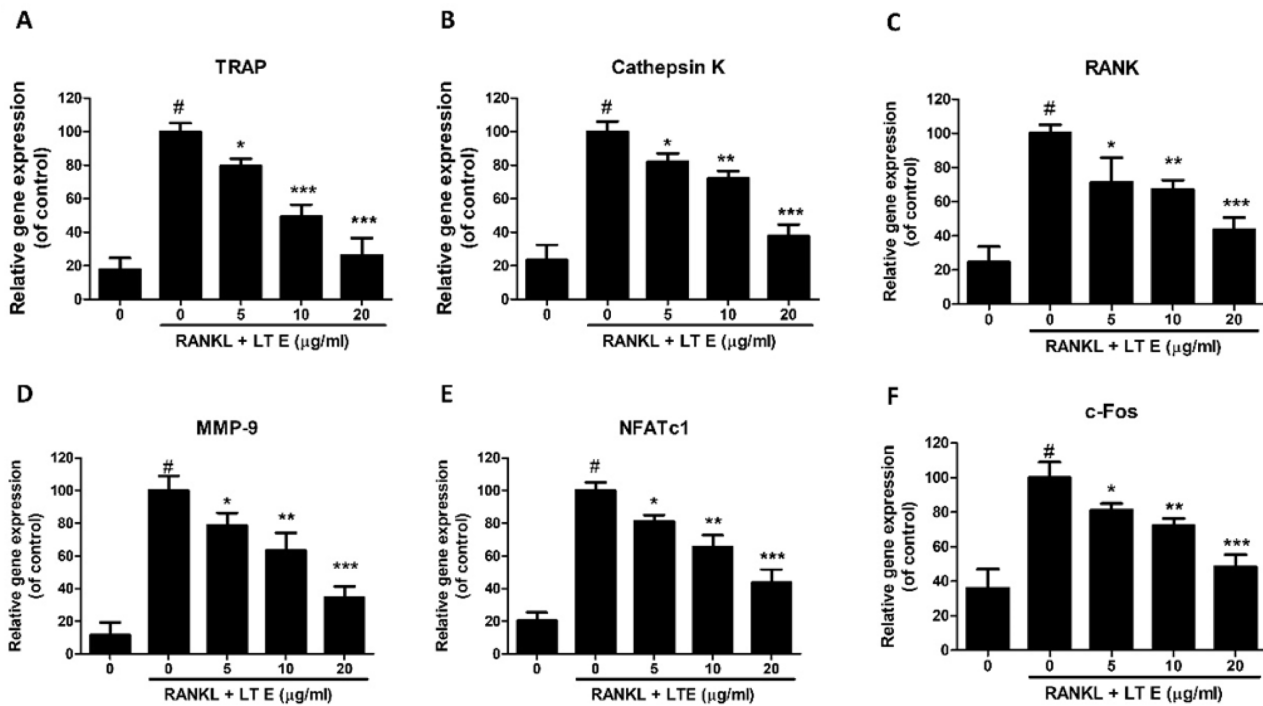


Fig. 3. LTE suppresses RANKL-stimulated osteoclastogenic gene expression in RAW 264.7 cells. 50 ng/mL RANKL was added to cells in the presence of 5, 10, and 20 µg/mL LTE for 3 days. (A-F) mRNA levels of Cts K, MMP-9, RANK, NFATc1, c-Fos, and TRAP genes were determined by reverse transcriptase-qPCR and compared with their levels in the untreated group. (β -actin was used as an internal control; $n = 3$. Results are presented as means \pm S.D. * $p < 0.05$, ** $p < 0.01$ vs. RANKL treated as control.

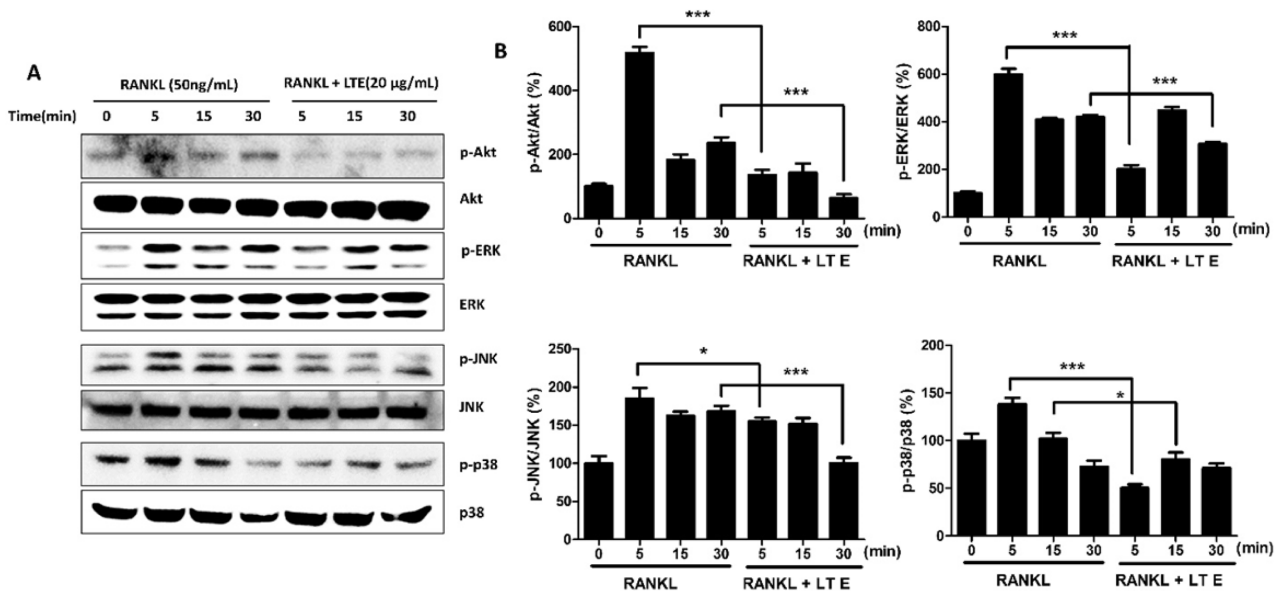


Fig. 4. LTE reduces RANKL-induced MAPKs/Akt pathway activation. (A) 20 µg/mL LTE was added to RAW264.7 cells for 30 min, and cells were then stimulated with 50 ng/mL RANKL for a defined time. (B) Proteins were analyzed by immunoblotting antibodies against p-p38/p38, p-JNK/JNK, p-ERK/ERK, and p-Akt/Akt. β -actin acted as an internal control; $n = 3$. Results are presented as means \pm S.D. * $p < 0.05$, ** $p < 0.01$, *** $p < 0.001$ vs. RANKL treated as control.

cells, phosphorylation of ERK1/2, JNK, and p38 proteins was considerably reduced (Fig. 4A, B). In RANKL-induced RAW264.7 cells, our findings show that LTE

suppresses osteoclast differentiation via downregulating MAPKs.

We also examined whether LTE might inhibit NFATc1,

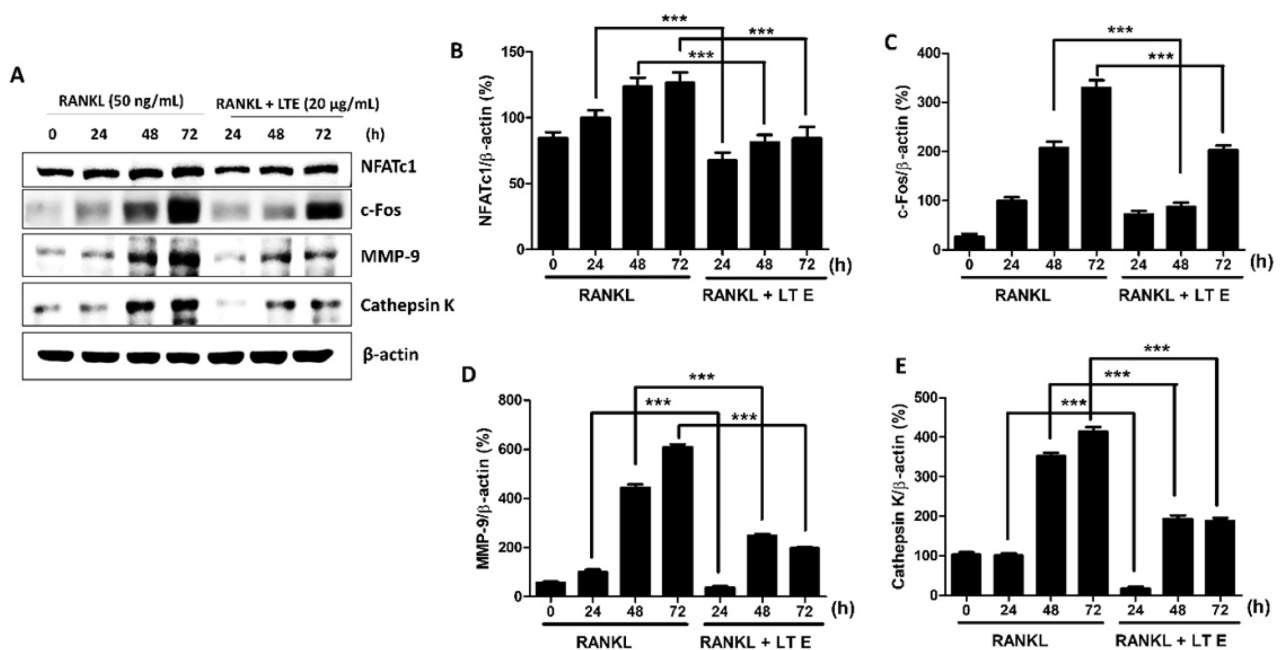


Fig. 5. Effect of LTE on RANKL-induced osteoclastogenic proteins expression. (A) RAW 264.7 cells were cultured in an osteoclastogenic medium with RANKL or LTE (20 $\mu\text{g}/\text{mL}$) for 6 days. (B) Western blot analysis examined the expression of NFATc1, c-Fos, MMP-9, and cathepsin K. β -actin acted as an internal control; $n = 3$. Results are presented as means \pm S.D. * $p < 0.05$, ** $p < 0.01$, *** $p < 0.001$ vs. RANKL treated as control.

a critical transcriptional regulator of osteoclast development.²² We also looked at c-Fos expression linked to osteoclast differentiation via NFATc1 downregulation. At a 20 $\mu\text{g}/\text{mL}$ concentration, RANKL dramatically enhanced the mRNA expression of NFATc1 and c-Fos, whereas LTE considerably lowered the transcription level of NFATc1 and c-Fos (Fig. 3E, F). Furthermore, a western blotting study demonstrated that RANKL enhanced NFATc1 and c-Fos protein expression, whereas treatment with 20 $\mu\text{g}/\text{mL}$ LTE significantly decreased NFATc1 and c-Fos protein expression for 3 days (Fig. 5A-C). LTE also inhibits the expression of MMP9 and Cts K protein expression, which are essential components during osteolysis (Fig. 5D, E). According to these findings, LTE decreases the transcriptional and translational expression of NFATc1 and c-Fos during osteoclast development and inhibits the expression of MMP9 and Cts K. NFATc1 and c-Fos are transcription factors required for osteoclastogenesis and differentiation of osteoclasts.²³ NFATc1 produces RANKL signaling information in osteoclasts as a downstream regulator of c-Fos, NF- κ B, and MAPKs.²⁴ NFATc1 stimulates the activation of NFATc1 and the transcription of osteoclast-specific genes such as TRAP, MMP-9, and Cts K via interacting with c-Fos.²⁵ LTE suppressed the expression of RANKL-induced NFATc1 and c-Fos in this investigation, consistent with earlier observations that

RANKL/RANK axis activation leads to downstream NFATc1 expression. LTE also inhibited the expression of c-Fos, NFATc1, RANK, MMP-9, Cts K, and TRAP, which are highly active genes in RANKL-induced osteoclastogenesis. More research in ovariectomized (OVX) mice or clinical trials is needed to better understand the underlying processes of LTE.

Finally, our findings show that LTE inhibits RANKL-induced osteoclast development in RAW 264.7 cells. LTE also inhibits the MAPKs pathway and reduces the production of transcription factors such as c-Fos and NFATc1. LTE appears to be a viable therapeutic therapy for osteolytic illnesses such as osteoporosis, Paget's disease, and osteogenesis imperfecta.

Acknowledgments

The authors thank the Jeonbuk National University Writing Center for its skilled proofreading service. This research was supported by Basic Science Research Program through the National Research Foundation of Korea (NRF), funded by the Ministry of Education (NRF-2021R111A3055927 to Soh Y), and Research Base Construction Fund Support Program funded by Jeonbuk National University in 2022. This paper was also supported by a grant from the Technology Innovation Pro-

gram (20012892) funded by the Ministry of Trade, Industry & Energy (MOTIE, Korea).

Conflict of Interest

The authors declare that there is no conflict of interest.

References

- (1) Boyle, W. J.; Simonet, W. S.; Lacey, D. L. *Nature* **2003**, *423*, 337–342.
- (2) Granchi, D.; Baldini, N.; Olivieri, F. M.; Caudarella, R. *Nutrients* **2019**, *11*, 2576.
- (3) Caetano-Lopes, J.; Canhao, H.; Fonseca, J. E. *Acta Reumatol. Port.* **2007**, *32*, 103–110.
- (4) Teitelbaum, S. L.; Ross, F. P. *Nat. Rev. Genet* **2003**, *4*, 638–649.
- (5) Kenkre, J.; Bassett, J. *Ann. Clin. Biochem.* **2018**, *55*, 308–327.
- (6) Crockett, J. C.; Mellis, D. J.; Scott, D. I.; Helfrich, M. H. *Osteoporos. Int.* **2011**, *22*, 1–20.
- (7) Wittrant, Y.; Théoleyre, S.; Chipoy, C.; Padrines, M.; Blanchard, F.; Heymann, D.; Rédini, F. *Biochim. Biophys. Acta.* **2004**, *1704*, 49–57.
- (8) Renema, N.; Navet, B.; Heymann, M. F.; Lezot, F.; Heymann, D. *Biosci. Rep.* **2016**, *36*, e00366.
- (9) Chen, X.; Wang, Z.; Duan, N.; Zhu, G.; Schwarz, E. M.; Xie, C. Osteoblast–osteoclast interactions. *Connect. Tissue Res.* **2018**, *59*, 99–107.
- (10) Yang, D. H.; Yang, M. Y. *Int. J. Mol. Sci.* **2019**, *20*, 2093.
- (11) Lee, Y. G.; Song, M. Y.; Cho, H.; Jin, J. S.; Park, B. H.; Bae, E. J. *Nutrients* **2022**, *14*, 3904.
- (12) Kim, N. H.; Heo, J. D.; Rho, J. R.; Yang, M. H.; Jeong, E. J. *Pharmacogn. Mag.* **2018**, *14*, 58–63.
- (13) Kim, N. H.; Heo, J. D.; Kim, T. B.; Rho, J. R.; Yang, M. H.; Jeong, E. J. *Biol. Pharm. Bull.* **2016**, *39*, 1022–1028.
- (14) Bae, M. J.; Karadeniz, F.; Oh, J. H.; Yu, G. H.; Jang, M. S.; Nam, K. H.; Seo, Y.; Kong, C. S. *Evid. Based Complement. Alternat. Med.* **2017**, *2017*, 6750274.
- (15) Lee, S. G.; Karadeniz, F.; Seo, Y.; Kong, C. S. *Molecules* **2017**, *22*, 1480.
- (16) Lee, Y. G.; Song, M. Y.; Cho, H.; Jin, J. S.; Park, B. H.; Bae, J. J. *Nutrients* **2022**, *14*, 3904.
- (17) Wilson, S. R.; Peters, C.; Saftig, P.; Bromme, D. Cathepsin K. *J. Biol. Chem.* **2009**, *284*, 2584–2592.
- (18) Takayanagi, H.; Kim, S.; Matsuo, K.; Suzuki, H.; Suzuki, T.; Sato, K.; Yokochi, T.; Oda, H.; Nakamura, K.; Ida, N.; Wagner, E. F.; Taniguchi, T. *Nature* **2002**, *416*, 744–749.
- (19) Yuan, F. L.; Xu, R. S.; Jiang, D. L.; He, X. L.; Su, Q.; Jin, C.; Li, X. *Bone* **2015**, *75*, 128–137.
- (20) Miyamoto, T.; Suda, T. *Keio J. Med.* **2003**, *52*, 1–7.
- (21) Lee, K.; Seo, I.; Choi, M. H.; Jeong, D. *Int. J. Mol. Sci.* **2018**, *19*, 3004.
- (22) Kim, J. H.; Kim, N. *J. Bone Metab.* **2014**, *21*, 233–241.
- (23) Grigoriadis, A. E.; Wang, Z. Q.; Cecchini, M. G.; Hofstetter, W.; Felix, R.; Fleisch, H. A.; Wagner, E. F. *Science* **1994**, *266*, 443–448.
- (24) Park, J. H.; Lee, N. K.; Lee, S. Y. *Mol. Cells* **2017**, *40*, 706–713.
- (25) Asagiri, M.; Sato, K.; Usami, T.; Ochi, S.; Nishina, H.; Yoshida, H.; Morita, I.; Wagner, E. F.; Mak, T. W.; Serfling, E.; Takayanagi, H. *J. Exp. Med.* **2005**, *202*, 1261–1269.

Received July 04, 2023

Revised November 28, 2023

Accepted December 15, 2023